

# SIEVING NONLINEAR INTERNAL WAVES IN SATELLITE IMAGES

Cho-Teng Liu<sup>1</sup>, Yen-Hsiang Chao<sup>1</sup>, Ming-Kuang Hsu<sup>2</sup> and Hsien-Wen Chen<sup>3</sup>

<sup>1</sup>Institute of Oceanography, National Taiwan University, Taipei, Taiwan, ROC 106, ctliu@ntu.edu.tw

<sup>2</sup>Northern Taiwan Institute of Science and Technology, Taipei, Taiwan, ROC 106, hsu.ming.kuang@gmail.com

<sup>3</sup>Department of Water Police, Central Police University, Taoyuan, Taiwan, ROC 106, una146@sun4.cpu.edu.tw

## ABSTRACT:

Nonlinear internal waves (NLIW) were studied as a unusual phenomena in the ocean decades ago. As the quality, quantity and variety of satellite images improve over decades, it is founded that NLIW is a ubiquitous phenomenon. Over the continental shelf of northern South China Sea (SCS), both optical and microwave images show that there are trains of NLIW packets near Dongsha Atoll (20.7N, 116.8E). Each packet contains several NLIW fronts. These NLIW packets are nearly parallel to each other and they are refracted, reflected or diffracted by the change of ocean bottom topography. Based on Korteweg de Vries (KdV) theory and the assumption that the bright/dark lines in the satellite images are centers of convergence/divergence of NLIW fronts, one may (1) sort NLIW packets in the same satellite image into groups of the same source, but generated at different tidal cycles, (2) relate NLIW packets in consecutive satellite images of one day apart, (3) locating faint signals of NLIW fronts in a satellite image. The NLIWs travel more than 100 km/day near Dongsha Atoll, with higher speed in deeper water. The bias and standard deviation of predicted location of NLIW front from its true location is about 1% and 5.1%, respectively.

**KEYWORDS:** Non-Linear Internal Waves, SAR, MODIS, South China Sea

## 1. INTRODUCTION

From satellite images of visible light (Fett and Rade, 1977; Bole et al., 1994), SAR (Synthetic Aperture Radar) in recent years (Liu et al., 1998; Hsu et al., 2000; Liu and Hsu, 2004; Liu et al., 2004), and MODIS (Moderate-resolution Imaging Spectroradiometer) images, one can find evidence of nonlinear internal waves (NLIW). Most of NLIWs in these satellite images were found over the continental shelf of South China Sea (SCS). Liu and Hsu (2004) collected hundreds of ERS-1/2, Radarsat SAR images and plot the distribution of NLIW in SCS (Fig. 1).

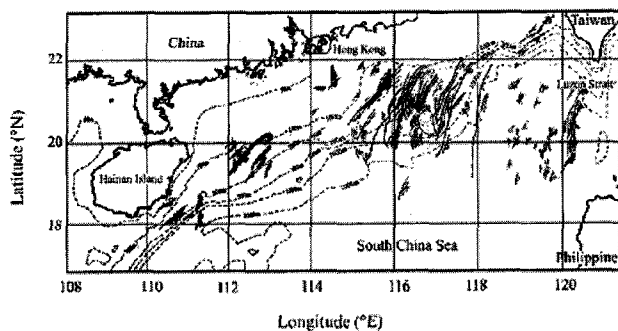


Fig. 1 Bathymetry and internal wave distribution map in the South China Sea (Liu and Hsu, 2004)

In the region of active NLIWs, like northern SCS, NLIWs will be refracted, reflected, or diffracted when passing different bottom topography after entering the continental shelf from deep water. In a satellite images, there are many packets of NLIW fronts (Fig. 2). It is not clear which fronts belong to the same packet, and which packets came from the same source region (i.e. they were generated at the same place but at different tidal cycle). If there are continuous images from satellites, one can track the location of each NLIW packet at different time, and categorize the NLIW packets according to their source region, generation mechanism, and study their phase relation with the tidal current. In most cases, the time lapse between two satellite images are too long, such that the location of a NLIW front in the new image can not be identified easily.

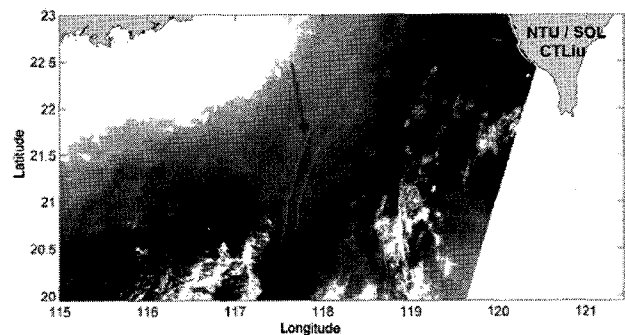


Fig.2 2003/05/07 Terra MODIS Image

Under the condition of non-continuous satellite images, one must know the propagation velocity of NLIW before sorting out the NLIW packets in different image were from the same source region.

It is impractical to monitor the propagation of NLIW over continental shelf. One will need many moorings to track a packet of NLIW, because NLIWs constantly change their shapes and propagating velocity. Usually, one uses numerical models to relate NLIW-like disturbance that were found in two moorings that were at 10s of km apart. Simulation requires assigning initial states, like the amplitude of NLIW, the thickness and density structure for the simplest 2-layer case.

If we do not have in situ measurement of layer thickness, the amplitude of NLIW, nor the propagation velocity, we may estimate the propagation speed of linear internal wave from hydrological data, and then estimate the NLIW propagation speed from the distance of bright band and dark band in SAR or MODIS images, based on the soliton theory of Korteweg - de Vries (KdV) (Liu et al., 2004).

## 2. METHOD

KdV equation is used to describe the propagation of slightly nonlinear IW in shallow water, and the water depth is much larger than the half width of NLIW. The equation and solution of KdV are (Liu et al., 2004):

$$A_t + C_1 A_x + \alpha A A_x + \gamma C_1 A_{xxx} = 0 \quad (1)$$

$$A(x,t) = A_0 \operatorname{sech}^2\left(\frac{x - C_1 t}{L}\right) \quad (2)$$

where  $A_0$  is the amplitude of NLIW,  $\alpha$  is the coefficient of nonlinear term,  $\gamma$  is the coefficient of dispersion term.

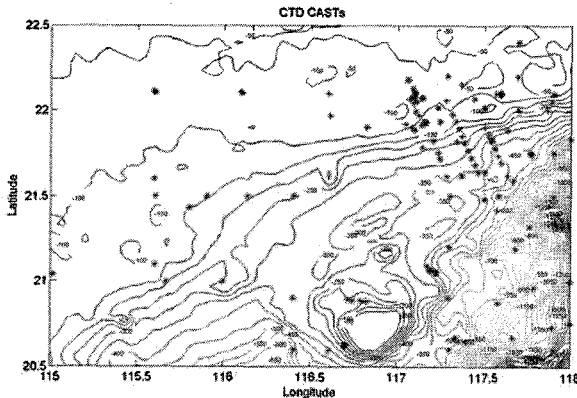


Fig. 3 Distribution of CTD casts

Due to uneven distribution of CTD casts (Fig. 3) over fast-change bathymetry, bilinear regression is used:

$$p = a x + b y + c x y + d \quad (3)$$

where  $p$  is temperature,  $x$  is longitude,  $y$  is latitude, and  $a, b, c, d$  are regression coefficients.

The distribution of hydrological data over a grid is derived with this regression method.

Under the assumption of linear, hydrostatic, frictionless and Boussinesq approximation, one may derive the characteristic equation for the vertical velocity  $\phi$  (Gill, 1982)

$$\frac{d^2 \phi_j}{dz^2} + \phi_j [N^2(z) - \omega^2] \lambda_j^2 = 0 \quad (4)$$

$$\lambda_j^2 = \frac{k^2}{\omega^2 - f^2} \quad (5)$$

$$k^2 = \lambda_j^2 \times (\omega^2 - f^2) \quad (6)$$

$\lambda$  is the eigen value,  $k$  is wave number,  $\omega$  is angular frequency of tides,  $f$  is Coriolis parameter, and  $N(z)$  is Brunt Vaisala frequency in Eq.(7).

$$N^2(z) = -\frac{g}{\rho} \frac{d\rho}{dz} \quad (7)$$

The boundary condition is  $\phi_j(0) = \phi_j(-H) = 0$

Normalization is  $\phi_{\max} = 1$ .

Let  $C_j$  represent the phase speed of  $j$ -th baroclinic mode. Because NLIW in SCS is dominated by the first baroclinic mode, we shall consider only  $C_1$ .

The coefficients of KdV equation are (Liu et al., 2004):

$$\alpha = \frac{3C_1 \int_{-H}^0 \frac{d^3 \phi}{dz^3} dz}{2 \int_{-H}^0 \frac{d^2 \phi}{dz^2} dz} \quad (8)$$

$$\gamma = \frac{\int_{-H}^0 \phi^2 dz}{2 \int_{-H}^0 \frac{d^2 \phi}{dz^2} dz} \quad (9)$$

The NLIW amplitude, half width and phase speed  $C_n$  satisfy the following equation (Liu, 1988) :

$$A_0 = \frac{12\gamma}{\alpha L^2} \quad (10)$$

$$C_n = C_1 + \frac{\alpha A_0}{3} \quad (11)$$

Because the short surface gravity wave travels slower than NLIWs and NLIWs has non-uniform horizontal orbital velocity, surface waves will be converged and diverged when NLIWs pass by, and result changes of surface roughness (Liu et al., 2000). Satellite images of SAR and MODIS show the changes of surface roughness that is caused by NLIW.

From in situ observation of NLIW amplitude, one may compute the propagation velocity  $C_n$  of NLIW (Osborne et al., 1980; Liu et al., 1985; Yang et al., 2004; Ramp et al., 2004).  $C_n$  can also be estimated from satellite images (Zhang et al., 2001; Hajji et al., 1999; Small, 1999; Liu et al., 2004):

$$D = 1.32L \quad (12)$$

where  $D$  is the distance between the brightest band and the darkest band, and  $L$  is the half width of NLIW.

From above method, we may compute the phase speed  $C_n$  of NLIW over the region of study, and contour the isolines of  $C_n$ , as in Fig. 4.

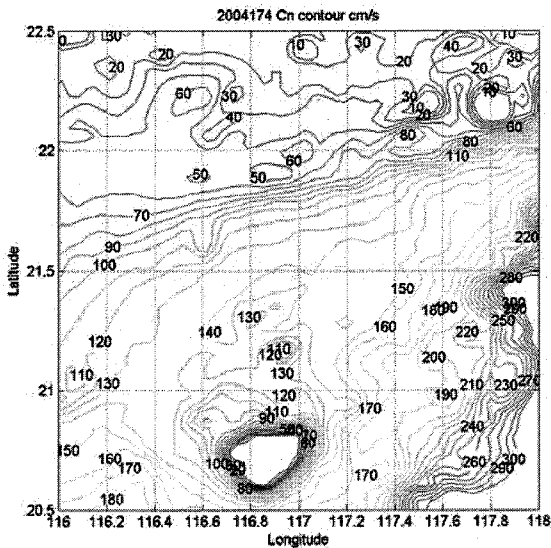


Fig. 4 Contour of Non-Linear Internal Wave phase speed  $C_n$

When a NLIW propagates through the region NE of Dongsha Atoll (116.8E, 20.7N), it will pass through regions of different  $C_n$  and be refracted according to Snell's Law.

Besides the refraction, waves will also be carried by ocean currents, especially the tidal current. Based on the barotropic tidal model by Egbert and Erofeeva (2002), the

location of NLIW front is further corrected with the model predicted tidal current velocity.

### 3. RESULT

In a MODIS image (Fig. 2), there are many packets of NLIW, with two very large packets at 117.7°E and 116.5°E that seem to come from Luzon Strait at different time. Are they related? What are the sources of other smaller packets. The period of occurrence of type-a NLIW from Luzon Strait, is about 24 hours (Ramp et al., 2004). Fig. 5 shows the predicted locations of NLIW fronts at 6 hour interval. With this prediction, we may pair NLIWs from the same source region (Luzon Strait), but at 24 hours apart. Other fronts in the image are from other sources.

One may also test this method with satellite images in the same day. For example, NLIW in 2005/05/01 is predicted from Aqua MODIS image at 05:10 and is compare against Envisat ASAR image at 14:13, to verify the prediction of NLIW propagation path (Fig. 6).

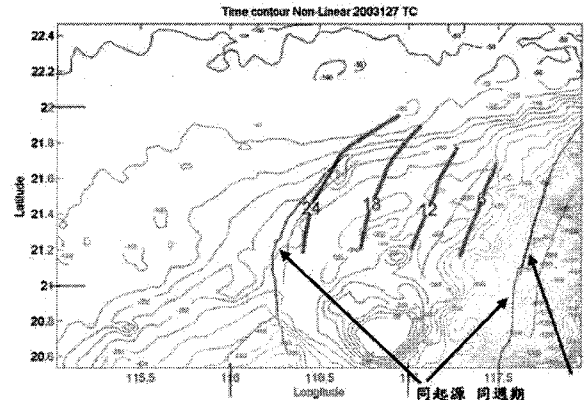


Fig. 5 Comparison of NLIW front location (blue lines) in 2003/05/07 Terra MODIS image of Channel 2, vs. those predicted (brown lines) from initial location (red lines)

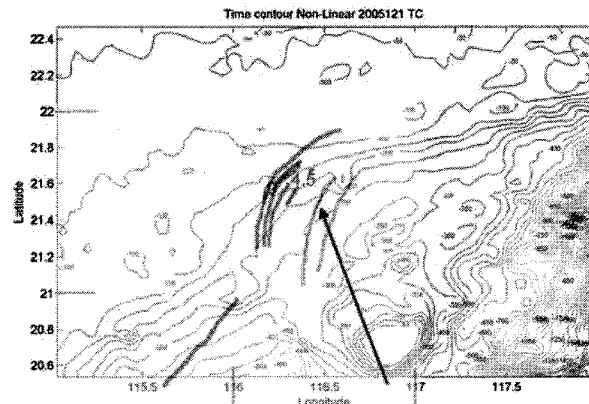


Fig. 6 Comparison of NLIW front location (blue lines) in ASAR image of 2005/05/01 14:13, vs. those predicted (brown lines) from initial location (red lines) in MODIS image 2005/05/01 satellite image

A useful application of predicting NLIW location is for confirmation of weak features (Fig. 7) in a satellite image. The surface signature of NLIW increases with NLIW

amplitude and decreases along propagation. One may predict the location of NLIW from an image of clear NLIW signature to predict its location one period earlier or later, in the same image, or in another image. This will help us confirm or reject weak NLIW signatures in a satellite image.

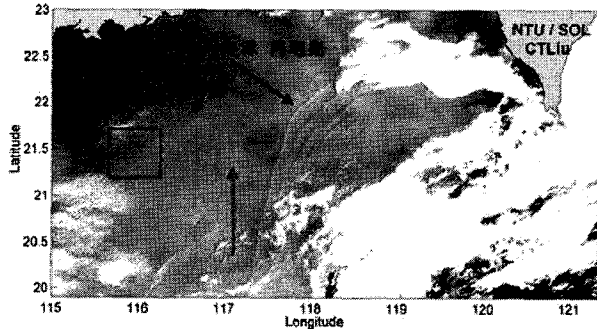


Fig. 7 2003/05/20 Terra MODIS Channel 2 image, it is suspected that there are NLIW signature in the blue frame, it is of the same origin like the NLIW at red arrow.

#### 4. CONCLUSIONS

There is no complete theory for explaining all NLIWs in SCS. This article uses the first order nonlinear KdV equation and tidal current model to predict the location and propagation of NLIW over continental shelf of SCS. The basic assumption includes negligible effect from mean current and from higher order nonlinearity, and the half-width of NLIW changes linearly between two fronts that are 24-hour apart. The error of predicted distance of propagation, or the propagation speed is about 5.1%. Ramp et al. (2004) plotted prediction of various models (Fig. 10) against observation at water depth 320 m (solid circles). The error is estimated about 12%.

This method may be used to estimate the location of NLIW as it propagates, and be used to distinguish NLIW packets of different origins, and to study the characteristics of individual NLIW front.

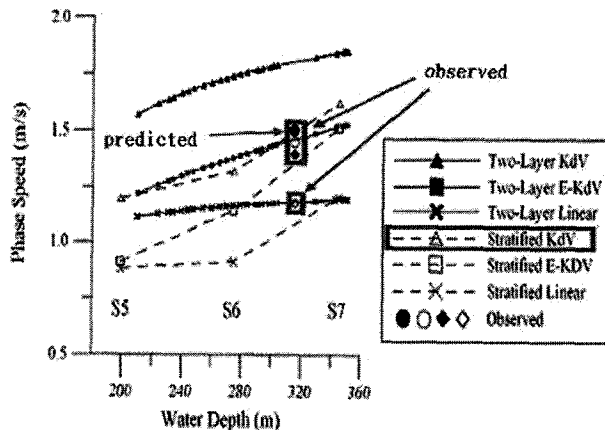


Fig. 9 Comparison between predicted (green) and observed (red) phase speed of NLIW (extracted from Ramp et al., 2004)

#### References:

- Bole, J. B., C. C. Ebbesmeyer and R. D. Romea, 1994. "Soliton Currents in the South China Sea: Measurement and Theoretical Modeling", Paper OTC 7417, presented at the 1994 Offshore Technology Conference, Houston, Texas, May 2-5, 1994, pp. 367-376.
- Egbert, G.D. and S.Y. Erofeeva, 2002. "Efficient inverse modeling of barotropic ocean tides", *J. Atmos. Oceanic Technol.*, 19(2), pp. 183-204.
- Fett, R. and K. Rabe, 1977. "Satellite observation of internal wave refraction in the South China Sea", *Geophys. Res. Lett.*, 4, pp. 189-191.
- Gill, A.E., 1982. "Atmosphere-Ocean Dynamics", Academic Press, San Diego, pp. 662
- Hajji, H., S. Sole and A. Ramamonjisoa, 1999. "Analysis and Prediction of Internal Waves Using SAR image and Non-linear model" www.meteomer.fr
- Hsu, M.K. and A. K. Liu, 2000. "Nonlinear internal waves in the South China Sea", *Can. J. of Rem. Sens.*, 26(2), pp. 72-81.
- Hsu, M. K., A. K. Liu and C. Liu, 2000. "A study of internal waves in the China Seas and Yellow Sea using SAR", *Cont. Shelf Res.*, 20, pp. 389-410.
- Liu, C-T, R. Pinkel, M-K Hsu, J. Klymak, H-W Chen, C. Villanoy, 2006. "Non-linear Internal Wave Giants from Luzon Strait", 2006, EOS (accepted)
- Liu, A. K., J. R. Apel and J. R. Holbrook, 1985. "Nonlinear internal wave Evolution in the Sulu Sea", *J. Phys. Oceanogr.*, 15, pp. 1613-1624.
- Liu, A. K., Y. S. Chang, M. K. Hsu and N. K. Liang, 1998. "Evolution of nonlinear internal waves in the East and South China Seas", *J. Geophys. Res.*, 103, pp. 7995-8008.
- Liu, A. K. and M. K. Hsu, 2004. "Internal wave study in the South China Sea using Synthetic Aperture Radar (SAR)", *Int. J. Rem. Sens.*, 10-20, 25, No. 7-8, pp. 1261-1264.
- Osborne, A. R. and T. L. Burch, 1980. "Internal Solitons in the Andaman Sea", *Science*, 208, pp. 451-460.
- Ramp, S.R., T. Y. Tang, T. F. Duda, J.F. Lynch, 2004. "Internal Solitons in the Northeastern South China Sea", *IEEE J. Ocean Eng.*, 29, pp. 1157-1181.
- Small, J., Z. Hallock, G. Pavey and J. C. Scott, 1999. "Observations of large amplitude internal waves at the Malin Shelf edge during SESAME 1995", *Cont. Shelf Res.*, 19, pp. 1389-1436.
- Zheng, Q., Y. Yuan, V. Klemas and X. H. Yan, 2001. "Theoretical expression for an ocean internal soliton synthetic aperture radar image and determination of the soliton characteristic half width", *J. Geophys. Res.*, 106, pp. 31415-31423.